

Research Paper

Characteristics of Vibrating Composite Stiffened Hypars with Cut-Out at Different Modes

Sarmila SAHOO

*Department of Civil Engineering
Heritage Institute of Technology
Kolkata-700107, India
e-mail: sarmila.sahoo@gmail.com*

Vibration characteristics of laminated composite stiffened hypar (hyperbolic paraboloid shell bounded by straight edges) with cut-out are analysed in terms of natural frequency and mode shapes. A finite element code is developed for the purpose by combining an eight noded curved shell element with a three noded curved beam element for stiffener. Finite element formulation is based on first order shear deformation theory and includes the effect of cross curvature. The isoparametric shell element used in the present model consists of eight nodes with five degrees of freedom per node while beam element has four degrees of freedom per node. The code is validated by solving benchmark problems available in the literature and comparing the results. The generalised Eigen value solution is chosen for the un-damped free vibration analysis. New results are presented for first five modes of natural frequency by varying boundary conditions, ply orientation and curvature of the shell. The results furnished here may be readily used by practicing engineers dealing with stiffened composite hypars with cut-outs.

Key words: free vibration; laminated composite; stiffened hypar shell; cut-out; first five modes.

NOTATIONS

- a, b – length and width of shell in plan,
- a', b' – length and width of cut-out in plan,
- b_{st} – width of stiffener in general,
- b_{sx}, b_{sy} – width of X and Y -stiffeners respectively,
- B_{sx}, B_{sy} – strain displacement matrix of stiffener element,
- c – rise of hypar shell,
- d_{st} – depth of stiffener in general,
- d_{sx}, d_{sy} – depth of X and Y -stiffeners respectively,
- $\{d_e\}$ – element displacement,
- e – eccentricity of stiffeners with respect to mid surface of shell,
- e_{sx}, e_{sy} – eccentricities of X and Y -stiffeners with respect to mid surface of shell,

- E_{11}, E_{22} – elastic moduli,
 G_{12}, G_{13}, G_{23} – shear moduli of a lamina with respect to 1, 2 and 3 axes of fibre,
 h – shell thickness,
 M_{sxx}, M_{syy} – moment resultants of stiffeners,
 M_x, M_y – moment resultants of shell,
 M_{xy} – torsion resultant,
 np – number of plies in a laminate,
 n_x, n_y – number of stiffeners along X and Y directions respectively,
 N_1-N_8 – shape functions,
 N_x, N_y – inplane force resultants,
 N_{sxx}, N_{syy} – axial force resultants of stiffeners,
 N_{xy} – inplane shear resultant,
 Q_x, Q_y – transverse shear resultant,
 Q_{sxxz}, Q_{syyz} – transverse shear resultants of stiffeners,
 R_{xy} – radii of cross curvature of hypar shell,
 T_{sxx}, T_{syy} – torsion resultants of stiffeners,
 u, v, w – translational degrees of freedom,
 u_{sx}, w_{sx} – axial and transverse translational degrees of freedom at each node of X -stiffener element,
 v_{sy}, w_{sy} – axial and transverse translational degrees of freedom at each node of Y -stiffener element,
 x, y, z – local co-ordinate axes,
 X, Y, Z – global co-ordinate axes,
 z_k – distance of bottom of the k th ply from mid-surface of a laminate,
 α, β – rotational degrees of freedom,
 α_{sx}, β_{sx} – rotational degrees of freedom at each node of X -stiffener element,
 α_{sy}, β_{sy} – rotational degrees of freedom at each node of Y -stiffener element,
 $\delta_{sxi}, \delta_{syi}$ – nodal displacement of stiffener element,
 $\varepsilon_x, \varepsilon_y$ – inplane strain component,
 $\gamma_{xy}, \gamma_{xz}, \gamma_{yz}$ – shearing strain components,
 ν_{12}, ν_{21} – Poisson's ratios,
 ξ, η, τ – isoparametric co-ordinates,
 ρ – density of material,
 σ_x, σ_y – inplane stress components,
 $\tau_{xy}, \tau_{xz}, \tau_{yz}$ – shearing stress components,
 ω – natural frequency,
 $\bar{\omega}$ – non-dimensional natural frequency; $\bar{\omega} = \omega a^2 (\rho/E_{22}h^2)^{1/2}$.

1. INTRODUCTION

Laminated composite shell structures characterized by high strength to weight ratio and reduced dead weight are used in different structures of many engineering fields like civil, mechanical, aerospace and others. In civil engineering application laminated composite shells are used as roofing units as these can cover large

column free areas. Among the different shell configurations, hypar shell (hyperbolic paraboloid shell bounded by straight edges) is very popular as roofing units due to their aesthetic elegance (Fig. 1). The shell surface being doubly ruled, it is very easy to construct and construction becomes faster. Roof structures are sometimes provided with cutout to allow entry of light, venting and to provide accessibility of parts of the structures, and also to alter the resonant frequency. Shells with cutout, stiffened along the margin are an efficient way to enhance the stiffness of the structure without adding much mass. These stiffeners slightly increase the structure weight but have effect on structural strength and stability. In practice, shell roofs may have different combinations of boundary conditions and a comprehensive study of free vibration characteristics of such structures is of practical interest.

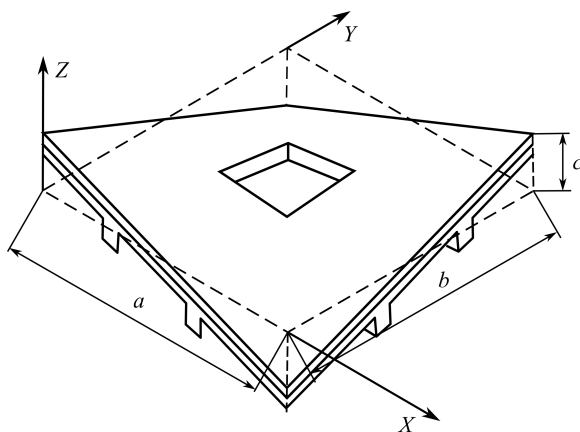


FIG. 1. Surface of a skewed hypar shell with cut-out. Surface equation: $z = \frac{4c}{ab} \left(x - \frac{a}{2}\right) \left(y - \frac{b}{2}\right)$.

Some of the earlier information regarding the behavior of doubly curved composite shells [1, 2] considered the practical boundary condition like corner point support and presented the frequency and mode shapes of spherical, circular cylindrical and hyperbolic paraboloidal (bounded by parabolas) shells. LIEW *et al.* [3] analyzed plates and shells for bending, buckling and vibration behavior using a super element. Point supported boundary conditions were also considered [4, 5]. QATU and LEISSA [6, 7] studied the free vibration behavior of doubly curved laminated composite shallow shells. QATU and LEISSA [8], and SIVASUBRAMONIAN *et al.* [9] studied the free vibration characteristics of doubly curved panels considering combinations of different boundary conditions. Liew and his colleagues [10–19] carried out extensive research work on the vibrations of different types of shell surfaces. The developments in the vibration of shallow shells reviewed in an excellent paper by LIEW *et al.* [20]. The fundamental frequencies of hypar shells with different boundary conditions were also reported [21, 22].

PRADYUMNA and BANDYOPADHYAY [23] reported the vibration characteristics of composite hypar shells based on HSDT but they did not considered higher modes, hence further improvement in these results have to be sought.

In this field of shell research, large number of research articles [24–37] is available. Free vibration aspects of stiffened shell panels with cut-out for six shell forms, viz., cylindrical, elliptic paraboloid, hyperbolic paraboloid, hypar, conoid and spherical shells have been studied using finite element method [38–44]. But analysis of stiffened shell with cut-out for modes of vibration other than fundamental mode are scanty in the literature. Though TOPAL [45], SRINIVASA *et al.* [46] presented the mode frequency analysis of laminated spherical shell but they did not consider hypar shells. Despite the engineering importance of cut-outs involved in composite panels, the number of research articles and reports in the subject topic are found to be limited. Some recent studies have addressed advanced aspects such as stochastic natural frequencies [47]. However, it is observed that there is no literature available on free vibration analysis of composite stiffened hypar shells with cut-out for other natural modes. In view of the above, a finite element model has been used in the present study for free vibration analysis of composite stiffened hypar shell with cut-out for first five natural modes. The analysis has been performed considering shallow shell assumptions. The effect of cross curvature is also included in the formulation. The present finite element model based on first order shear deformation theory is applied to solve many practical problems of laminated composite stiffened hypar shells considering different boundary conditions, laminations and curvature of shell.

2. MATHEMATICAL FORMULATION

A laminated composite hypar shell of uniform thickness h (Fig. 1) and radius of cross curvature R_{xy} is considered. Keeping the total thickness the same, the thickness may consist of any number of thin laminae each of which may be arbitrarily oriented at an angle θ with reference to the X -axis of the co-ordinate system. The constitutive equations for the shell are given by (a list of notations is separately given):

$$(2.1) \quad \{F\} = [E]\{\varepsilon\},$$

where

$$\{F\} = \{ N_x, N_y, N_{xy}, M_x, M_y, M_{xy}, Q_x, Q_y \}^T,$$

$$[E] = \begin{bmatrix} [A] & [B] & [0] \\ [B] & [D] & [0] \\ [0] & [0] & [S] \end{bmatrix}, \quad \{\varepsilon\} = \{ \varepsilon_x^0, \varepsilon_y^0, \gamma_{xy}^0, k_x, k_y, k_{xy}, \gamma_{xz}^0, \gamma_{yz}^0 \}^T.$$

The force and moment resultants are expressed as

$$(2.2) \quad \left\{ N_x, N_y, N_{xy}, M_x, M_y, M_{xy}, Q_x, Q_y \right\}^T \\ = \int_{-h/2}^{h/2} \left\{ \sigma_x, \sigma_y, \tau_{xy}, \sigma_z \cdot z, \sigma_y \cdot z, \tau_{xy} \cdot z, \tau_{xz}, \tau_{yz} \right\}^T dz.$$

The submatrices $[A]$, $[B]$, $[D]$ and $[S]$ of the elasticity matrix $[E]$ are functions of Young's moduli, shear moduli and the Poisson's ratio of the laminates. They also depend on the angle which the individual lamina of a laminate makes with the global X -axis. The detailed expressions of the elements of the elasticity matrix are available in several references including VASILIEV *et al.* [48] and QATU [49].

The strain-displacement relations on the basis of improved first order approximation theory for thin shell [50] are established as

$$(2.3) \quad \left\{ \varepsilon_x, \varepsilon_y, \gamma_{xy}, \gamma_{xz}, \gamma_{yz} \right\}^T = \left\{ \varepsilon_x^0, \varepsilon_y^0, \gamma_{xy}^0, \gamma_{xz}^0, \gamma_{yz}^0 \right\}^T \\ + z \left\{ k_x, k_y, k_{xy}, k_{xz}, k_{yz} \right\}^T,$$

where the first vector is the mid-surface strain for a hypar shell and the second vector is the curvature.

2.1. Finite element formulation for shell

An eight-noded curved quadratic isoparametric finite element is used for hypar shell analysis. The five degrees of freedom taken into consideration at each node are u , v , w , α , β . The following expressions establish the relations between the displacement at any point with respect to the co-ordinates ξ and η and the nodal degrees of freedom.

$$(2.4) \quad u = \sum_{i=1}^8 N_i u_i, \quad v = \sum_{i=1}^8 N_i v_i, \quad w = \sum_{i=1}^8 N_i w_i, \\ \alpha = \sum_{i=1}^8 N_i \alpha_i, \quad \beta = \sum_{i=1}^8 N_i \beta_i,$$

where the shape functions derived from a cubic interpolation polynomial [50] are:

$$(2.5) \quad N_i = (1 + \xi\xi_i)(1 + \eta\eta_i)(\xi\xi_i + \eta\eta_i - 1)/4, \quad \text{for } i = 1, 2, 3, 4, \\ N_i = (1 + \xi\xi_i)(1 - \eta^2)/2, \quad \text{for } i = 5, 7, \\ N_i = (1 + \eta\eta_i)(1 - \xi^2)/2, \quad \text{for } i = 6, 8.$$

The generalized displacement vector of an element is expressed in terms of the shape functions and nodal degrees of freedom as:

$$(2.6) \quad [u] = [N]\{d_e\},$$

i.e.

$$\{u\} = \begin{Bmatrix} u \\ v \\ w \\ \alpha \\ \beta \end{Bmatrix} = \sum_{i=1}^8 \begin{bmatrix} N_i & & & & \\ & N_i & & & \\ & & N_i & & \\ & & & N_i & \\ & & & & N_i \end{bmatrix} \begin{Bmatrix} u_i \\ v_i \\ w_i \\ \alpha_i \\ \beta_i \end{Bmatrix}.$$

2.1.1. Element stiffness matrix. The strain-displacement relation is given by

$$(2.7) \quad \{\varepsilon\} = [B]\{d_e\},$$

where

$$(2.8) \quad [B] = \sum_{i=1}^8 \begin{bmatrix} N_{i,x} & 0 & 0 & 0 & 0 \\ 0 & N_{i,y} & 0 & 0 & 0 \\ N_{i,y} & N_{i,x} & -2N_i/R_{xy} & 0 & 0 \\ 0 & 0 & 0 & N_{i,x} & 0 \\ 0 & 0 & 0 & 0 & N_{i,y} \\ 0 & 0 & 0 & N_{i,y} & N_{i,x} \\ 0 & 0 & N_{i,x} & N_i & 0 \\ 0 & 0 & N_{i,y} & 0 & N_i \end{bmatrix}.$$

The element stiffness matrix is

$$(2.9) \quad [K_e] = \iint [B]^T [E] [B] dx dy.$$

2.1.2. Element mass matrix. The element mass matrix is obtained from the integral

$$(2.10) \quad [M_e] = \iint [N]^T [P] [N] dx dy,$$

where

$$[N] = \sum_{i=1}^8 \begin{bmatrix} N_i & 0 & 0 & 0 & 0 \\ 0 & N_i & 0 & 0 & 0 \\ 0 & 0 & N_i & 0 & 0 \\ 0 & 0 & 0 & N_i & 0 \\ 0 & 0 & 0 & 0 & N_i \end{bmatrix}, \quad [P] = \sum_{i=1}^8 \begin{bmatrix} P & 0 & 0 & 0 & 0 \\ 0 & P & 0 & 0 & 0 \\ 0 & 0 & P & 0 & 0 \\ 0 & 0 & 0 & I & 0 \\ 0 & 0 & 0 & 0 & I \end{bmatrix},$$

in which

$$(2.11) \quad P = \sum_{k=1}^{np} \int_{z_{k-1}}^{z_k} \rho dz \quad \text{and} \quad I = \sum_{k=1}^{np} \int_{z_{k-1}}^{z_k} z \rho dz.$$

2.2. Finite element formulation for stiffener

Three noded curved isoparametric beam elements (Fig. 2) are used to model the stiffeners, which are taken to run only along the boundaries of the shell elements. In the stiffener element, each node has four degrees of freedom i.e. u_{sx} , w_{sx} , α_{sx} and β_{sx} for X -stiffener and v_{sy} , w_{sy} , α_{sy} and β_{sy} for Y -stiffener. The generalized force-displacement relation of stiffeners can be expressed as:

$$(2.12) \quad \begin{aligned} X\text{-stiffener: } \{F_{sx}\} &= [D_{sx}] \{\varepsilon_{sx}\} = [D_{sx}] [B_{sx}] \{\delta_{sxi}\}, \\ Y\text{-stiffener: } \{F_{sy}\} &= [D_{sy}] \{\varepsilon_{sy}\} = [D_{sy}] [B_{sy}] \{\delta_{syi}\}, \end{aligned}$$

where

$$\begin{aligned} \{F_{sx}\} &= [N_{sxx} \quad M_{sxx} \quad T_{sxx} \quad Q_{sxxz}]^T, \\ \{\varepsilon_{sx}\} &= [u_{sxx} \quad \alpha_{sxx} \quad \beta_{sxx} \quad (\alpha_{sx} + w_{sx,x})]^T \end{aligned}$$

and

$$\begin{aligned} \{F_{sy}\} &= [N_{syy} \quad M_{syy} \quad T_{syy} \quad Q_{syyz}]^T, \\ \{\varepsilon_{sy}\} &= [v_{syy} \quad \beta_{syy} \quad \alpha_{syy} \quad (\beta_{sy} + w_{sy,y})]^T. \end{aligned}$$

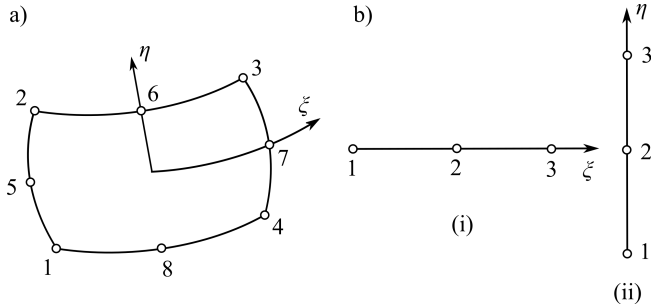


FIG. 2. a) Eight noded shell element; b) three noded stiffener element:
(i) X -stiffener, (ii) Y -stiffener.

The generalized displacements of the Y -stiffener and the shell are related by the transformation matrix $\{\delta_{syi}\} = [T] \{\delta\}$ where

$$[T] = \begin{bmatrix} 1 + \frac{e}{R_y} & \text{symmetric} & & \\ 0 & 1 & & \\ 0 & 0 & 1 & \\ 0 & 0 & 0 & 1 \end{bmatrix}.$$

This transformation is required due to curvature of Y -stiffener and $\{\delta\}$ is the appropriate portion of the displacement vector of the shell excluding the displacement component along the X -axis.

Elasticity matrices are as follows:

$$[D_{sx}] = \begin{bmatrix} A_{11}b_{sx} & B'_{11}b_{sx} & B'_{12}b_{sx} & 0 \\ B'_{11}b_{sx} & D'_{11}b_{sx} & D'_{12}b_{sx} & 0 \\ B'_{12}b_{sx} & D'_{12}b_{sx} & \frac{1}{6}(Q_{44} + Q_{66})d_{sx}b_{sx}^3 & 0 \\ 0 & 0 & 0 & b_{sx}S_{11} \end{bmatrix},$$

$$[D_{sy}] = \begin{bmatrix} A_{22}b_{sy} & B'_{22}b_{sy} & B'_{12}b_{sy} & 0 \\ B'_{22}b_{sy} & \frac{1}{6}(Q_{44} + Q_{66})b_{sy} & D'_{12}b_{sy} & 0 \\ B'_{12}b_{sy} & D'_{12}b_{sy} & D'_{11}d_{sy}b_{sy}^3 & 0 \\ 0 & 0 & 0 & b_{sy}S_{22} \end{bmatrix},$$

where

$$(2.13) \quad D'_{ij} = D_{ij} + 2eB_{ij} + e^2A_{ij}, \quad B'_{ij} = B_{ij} + eA_{ij},$$

and A_{ij} , B_{ij} , D_{ij} and S_{ij} are explained in an earlier paper by SAHOO and CHAKRAVORTY [29]. Here, considering the stiffener as moderately thick, the shear correction factor is taken as $5/6$. The sectional parameters are calculated with respect to the mid-surface of the shell by which the effect of eccentricities of stiffeners is automatically included. The element stiffness matrices are of the following forms

$$(2.14) \quad \begin{aligned} \text{for } X\text{-stiffener: } [K_{xe}] &= \int [B_{sx}]^T [D_{sx}] [B_{sx}] dx, \\ \text{for } Y\text{-stiffener: } [K_{ye}] &= \int [B_{sy}]^T [D_{sy}] [B_{sy}] dy. \end{aligned}$$

The integrals are converted to isoparametric co-ordinates and are carried out by 2-point Gauss quadrature. Finally, the element stiffness matrix of the stiffened shell is obtained by appropriate matching of the nodes of the stiffener and shell elements through the connectivity matrix and is given as:

$$(2.15) \quad [K_e] = [K_{she}] + [K_{xe}] + [K_{ye}].$$

The element stiffness matrices are assembled to get the global matrices.

2.2.1. *Element mass matrix.* The element mass matrix for shell is obtained from the integral

$$(2.16) \quad [M_e] = \iint [N]^T [P] [N] dx dy,$$

where

$$[N] = \sum_{i=1}^8 \begin{bmatrix} N_i & 0 & 0 & 0 & 0 \\ 0 & N_i & 0 & 0 & 0 \\ 0 & 0 & N_i & 0 & 0 \\ 0 & 0 & 0 & N_i & 0 \\ 0 & 0 & 0 & 0 & N_i \end{bmatrix}, \quad [P] = \sum_{i=1}^8 \begin{bmatrix} P & 0 & 0 & 0 & 0 \\ 0 & P & 0 & 0 & 0 \\ 0 & 0 & P & 0 & 0 \\ 0 & 0 & 0 & I & 0 \\ 0 & 0 & 0 & 0 & I \end{bmatrix},$$

in which

$$(2.17) \quad P = \sum_{k=1}^{np} \int_{z_{k-1}}^{z_k} \rho dz \quad \text{and} \quad I = \sum_{k=1}^{np} \int_{z_{k-1}}^{z_k} z \rho dz.$$

Element mass matrix for stiffener element

$$(2.18) \quad \begin{aligned} [M_{sx}] &= \iint [N]^T [P] [N] dx \quad \text{for } X\text{-stiffener,} \\ [M_{sy}] &= \iint [N]^T [P] [N] dy \quad \text{for } Y\text{-stiffener.} \end{aligned}$$

Here, $[N]$ is a 3×3 diagonal matrix

$$[P] = \sum_{i=1}^3 \begin{bmatrix} \rho b_{sx} d_{sx} & 0 & 0 & 0 \\ 0 & \rho b_{sx} d_{sx} & 0 & 0 \\ 0 & 0 & \frac{\rho b_{sx} d_{sx}^2}{12} & 0 \\ 0 & 0 & 0 & \frac{\rho (b_{sx} d_{sx}^3 + b_{sx}^3 d_{sx})}{12} \end{bmatrix} \quad \text{for } X\text{-stiffener,}$$

$$[P] = \sum_{i=1}^3 \begin{bmatrix} \rho b_{sy} d_{sy} & 0 & 0 & 0 \\ 0 & \rho b_{sy} d_{sy} & 0 & 0 \\ 0 & 0 & \frac{\rho b_{sy} d_{sy}^2}{12} & 0 \\ 0 & 0 & 0 & \frac{\rho (b_{sy} d_{sy}^3 + b_{sy}^3 d_{sy})}{12} \end{bmatrix} \quad \text{for } Y\text{-stiffener.}$$

The mass matrix of the stiffened shell element is the sum of the matrices of the shell and the stiffeners matched at the appropriate nodes

$$(2.19) \quad [M_e] = [M_{she}] + [M_{xe}] + [M_{ye}].$$

The element mass matrices are assembled to get the global matrices.

2.3. Modeling the cut-out

The code developed can take the position and size of cut-out as input. The program is capable of generating non uniform finite element mesh all over the shell surface. So the element size is gradually decreased near the cut-out margins. One such typical mesh arrangement is shown in Fig. 3. Such finite element mesh is redefined in steps and a particular grid is chosen to obtain the fundamental frequency when the result does not improve by more than one percent on further refining. Convergence of results is ensured in all the problems taken up here. In the cut-out region, the mass matrix and stiffness matrix of the shell elements are considered to be null. The same has been appropriately implemented in the FE code by considering the thickness of the shell in that region to be negligible.

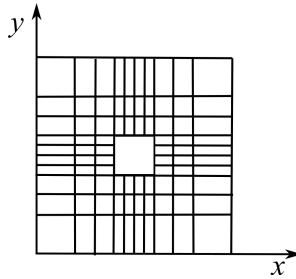


FIG. 3. Typical 10×10 non-uniform mesh arrangement drawn to scale.

2.4. Solution procedure for free vibration analysis

The free vibration analysis involves determination of natural frequencies from the condition

$$(2.20) \quad |[K] - \omega^2[M]| = 0.$$

This is a generalized eigen value problem and is solved by the subspace iteration algorithm.

3. VALIDATION STUDY AND NUMERICAL PROBLEMS

The results of Table 1 show that the agreement of present results with the earlier ones is excellent and the correctness of the stiffener formulation is established. Free vibration of simply supported and clamped hypar shell with $(0/90)_4$ shell with cut-outs is also considered. The fundamental frequencies of hypar shell with cut-out obtained by the present method agree well with those reported by CHAKRAVORTY *et al.* [21] as evident from Table 2, establishing the correctness of the cut-out formulation. Thus it is evident that the finite element model proposed here can successfully analyse vibration problems of stiffened skewed hypar composite shells with cut-out which is reflected by close agreement of present results with benchmark ones. The present approach uses the improved first order approximation theory for thin shells [52] considering the radius of cross curvature. For this class of thin shells, a shear correction factor of unity is found to yield good results. It is observed that the results remain the same when analysis is repeated with the commonly used shear correction factor of $\pi/\sqrt{12}$.

Table 1. Natural frequencies [Hz] of centrally stiffened clamped square plate.

Mode no.	MUKHERJEE and MUKHOPADHYAY [51]	NAYAK and BANDYOPADHYAY [25]		Present method
		N8(FEM)	N9(FEM)	
1	711.8	725.2	725.1	733

$a = b = 0.2032$ m, thickness = 0.0013716 m, stiffener depth = 0.0127 m, stiffener width = 0.00635 m, stiffener eccentric at bottom, material property: $E = 6.87 \cdot 10^{10}$ N/m², $\nu = 0.29$, $\rho = 2823$ kg/m³.

Table 2. Non-dimensional fundamental frequencies ($\bar{\omega}$) for hypar shells (lamination $(0/90)_4$) with concentric cut-outs.

a'/a	CHAKRAVORTY <i>et al.</i> [21]		Present finite element model					
	Simply supported	Clamped	Simply supported			Clamped		
			8×8	10×10	12×12	8×8	10×10	12×12
0.0	50.829	111.600	50.573	50.821	50.825	111.445	111.592	111.612
0.1	50.769	110.166	50.679	50.758	50.779	109.987	110.057	110.233
0.2	50.434	105.464	50.323	50.421	50.400	105.265	105.444	105.443
0.3	49.165	101.350	49.045	49.157	49.178	101.110	101.340	101.490
0.4	47.244	97.987	47.132	47.242	47.141	97.670	97.985	97.991

$a/b = 1$, $a/h = 100$, $a'/b' = 1$, $c/a = 0.2$; $E_{11}/E_{22} = 25$, $G_{23} = 0.2E_{22}$, $G_{13} = G_{12} = 0.5E_{22}$, $\nu_{12} = \nu_{21} = 0.25$.

Laminated composite stiffened hypar shells with cut-out is analysed to study the behaviour of the shell under free vibration at higher mode for different para-

metric variation. The cut-outs are placed concentrically on the shell surface. The stiffeners are placed along the cut-out periphery and extended up to the edge of the shell. The material and geometric properties of the shells are: $a/b = 1$, $a/h = 100$, $a'/b' = 1$, $a'/a = 0.2$, $c/a = 0.2$, $E_{11}/E_{22} = 25$, $G_{23} = 0.2E_{22}$, $G_{13} = G_{12} = 0.5E_{22}$, $\nu_{12} = \nu_{21} = 0.25$, $\rho = 100 \text{ N} \cdot \text{s}^2/\text{m}^4$ unless otherwise specified. Different type of symmetric and antisymmetric cross and angle ply laminates with different lamination angle is considered.

The different boundary conditions which are used in the present analysis are CCCC, CCSS, SSCC, CSCS, SCSC, SSSS, CCFE, FFCC and CFCF. The boundary conditions are designated as: C for clamped, S for simply supported and F for free edges. The four edges are considered in an anticlockwise order from the edge $x = 0$. For example a shell with CSCS boundary is clamped along $x = 0$, simply supported along $y = 0$ and clamped along $x = a$ and simply supported along $y = b$. Numerical analyses are also performed to determine the effect of curvature on non-dimensional frequency by varying $c/a = 0.2, 0.15, 0.1$, and 0.05 .

4. RESULTS AND DISCUSSIONS

4.1. *Effect of number and arrangement of boundary constraints on higher mode frequencies at different lamination stacking sequences*

Table 3 presents the non-dimensional frequencies for shells with different laminations and boundary conditions. To facilitate the interpretation of results the boundary conditions are divided into three groups. Group I consists of commonly encountered edge conditions which are clamped and simply supported. Each of the boundary conditions included in either of Group II and Group III has equal number of support constraints. On examining the results it is evident that the frequencies for all the laminations for first five modes depend on the number of boundary constraints. With increase in number of boundary constraints frequencies increase. Further it is noticed that for two layered laminates for Group I boundary conditions, angle ply shells show better performance than cross ply laminates but reverse is the case for Group III shells. For Group II shells both cross ply and angle ply shells show better performances from 1st to 5th mode. It is also evident from Table 3 that with increase in number of layers angle ply shells perform better than their cross ply counterpart, except some few cases. This is true for Group I and Group II shells but for Group III shells except a very few cases cross ply shells are better choices. These are true for first five natural modes.

Among Group II boundary conditions, CCSS performs better than CSCS shells for cross ply shells. For angle ply shells, CCSS shell performs better at 1st

Table 3. Non-dimensional frequencies $\bar{\omega}$ for different laminations of laminated composite stiffened hypar shell with cut-out for different boundary conditions on higher mode.

θ [°]	Mode	Group I		Group II		Group III	
		CCCC	SSSS	CCSS	CSCS	CCFF	CFCF
0/90	1	98.018	26.637	85.438	49.438	44.250	34.587
	2	108.446	26.929	91.838	76.142	52.083	61.940
	3	109.370	39.897	93.835	97.696	75.362	71.091
	4	119.423	42.461	103.232	102.429	77.192	76.053
	5	125.111	57.209	111.447	105.696	79.180	90.241
45/-45	1	120.698	37.986	83.906	49.165	27.561	26.910
	2	124.864	38.107	86.901	79.967	31.568	50.815
	3	125.550	60.215	93.530	113.990	54.854	54.034
	4	142.375	74.380	100.425	119.097	58.839	62.302
	5	180.017	96.224	117.059	119.229	66.271	82.723
0/90/0	1	100.702	40.793	87.276	47.510	43.943	22.040
	2	109.903	56.046	94.274	66.005	56.146	44.861
	3	117.771	57.826	101.721	90.226	73.599	75.056
	4	127.017	76.016	105.475	95.401	79.927	75.230
	5	127.127	88.721	112.081	108.090	85.013	76.614
45/-45/45	1	142.317	53.814	99.785	72.082	34.008	37.830
	2	149.189	55.274	108.133	113.228	37.943	59.124
	3	155.431	83.546	109.827	138.565	59.926	62.084
	4	159.182	106.898	128.808	143.016	67.858	80.642
	5	200.078	129.254	149.427	144.652	74.376	91.550
0/90/0/90	1	101.746	48.701	94.487	65.309	49.317	51.795
	2	117.561	48.995	97.755	87.723	59.477	71.901
	3	118.346	80.970	101.568	110.525	81.850	78.391
	4	134.043	89.063	121.367	115.587	85.988	88.043
	5	151.843	103.765	126.195	120.032	87.161	100.779
45/-45/45/-45	1	143.534	54.131	96.560	71.356	31.861	37.875
	2	157.273	54.182	113.940	113.115	36.583	62.076
	3	158.121	86.637	116.915	145.381	62.488	65.217
	4	165.640	106.252	127.234	146.878	68.768	83.822
	5	216.514	135.294	155.055	150.707	77.731	100.095
0/90/0/90/0	1	102.336	45.490	94.328	57.234	48.607	38.823
	2	114.740	55.612	97.220	82.655	59.331	65.989
	3	125.389	74.322	105.417	109.061	81.196	78.763
	4	138.143	91.929	116.855	113.620	83.160	83.759
	5	138.925	105.747	124.153	114.241	91.756	93.516

and 2nd modes, but the reverse is the case for 3rd to 5th modes. A more careful observation suggests that among Group III shells when numbers of layers are less CCFE performs better but with increase in number of layers performance of CFCF shells are improved. Hence lamination order may influence the frequency of stiffened composite shell with cut-out more significantly than its boundary conditions.

The typical mode shapes corresponding to the first five modes of vibration are plotted in Fig. 4 for cross ply and angle ply shells respectively. The normalized

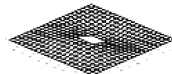
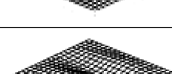
θ [°]	Mode	CCCC	CCSS	CFCF
0/90	1			
	2			
	3			
	4			
	5			
45/-45	1			
	2			
	3			
	4			
	5			

FIG. 4. Mode shapes for cross ply and angle ply shells for different boundary conditions for first five modes.

displacements are drawn with the shell mid-surface as the reference for all the support condition and for all the lamination used here. The fundamental mode is clearly a bending mode for all the boundary condition for cross ply and angle ply shell. At higher modes of vibration, mode shapes do not change to a great extent. Most of the mode shapes are in bending mode. It is found that for first five modes, nature of the mode shapes is somewhat similar, only the crest and trough position changes.

4.2. *Effect of lamination angle on symmetrically laminated shells*

Table 4 contains the non-dimensional frequency values for different symmetric laminates by varying the lamination angle and boundary conditions. It is observed from the results, with the increase in number of layers frequencies increase marginally from three layered to four layered shells. But with further increase in number of layers does not come to any effective benefit except CSCS and CFCF shells. This is expected as increasing the number of layers will result in reduced bending-stretching coupling and will increase the shell stiffness, till on increasing the number of layers the material becomes quasi-isotropic. Beyond that, increase in the number of layers will not improve the frequency to any extent. Rather, $(0/\theta)_s$ lamination exhibit reasonably good performance and may be adopted for all practical purposes. It is also observed that except for CCCC shells, where $\theta = 45^\circ$ yields the highest values of frequency but for all other

Table 4. Non-dimensional $\bar{\omega}$ frequencies for symmetric laminated composite stiffened hypar shell with cut-out with different boundary condition.

Boundary Condition	θ [°]	$(0/\theta/0)$	$(0/\theta)_s$	$(0/\theta/0)_s$	$[(0/\theta)_2]_s$
CCCC	0	92.874	93.093	93.526	93.093
	15	110.434	114.779	112.219	115.791
	30	120.993	122.546	123.193	123.201
	45	121.153	122.941	124.570	124.686
	60	117.064	118.771	121.600	121.632
	75	111.024	113.132	117.109	116.898
	90	100.702	102.030	102.571	102.587
CCSS	0	81.037	81.437	82.220	81.437
	15	84.473	85.188	86.148	85.424
	30	87.443	88.284	89.642	88.863
	45	88.839	89.657	91.149	90.260
	60	89.033	89.950	91.663	90.757
	75	87.885	89.911	92.831	91.997
	90	87.276	90.964	95.544	95.333

Table 4. [Cont.]

Boundary Condition	θ [°]	$(0/\theta/0)$	$(0/\theta)_S$	$(0/\theta/0)_S$	$[(0/\theta)_2]_S$
CSCS	0	39.747	39.935	40.302	39.939
	15	43.082	43.983	44.378	44.507
	30	47.388	49.570	50.896	51.678
	45	50.529	54.464	57.362	59.018
	60	52.420	58.216	62.162	64.869
	75	50.642	57.051	62.272	65.107
	90	47.510	53.208	60.222	62.180
SSSS	0	32.418	32.543	32.837	32.547
	15	34.688	35.396	35.853	35.964
	30	37.607	39.215	40.577	41.047
	45	39.729	42.274	44.529	45.304
	60	41.439	44.707	47.165	48.213
	75	41.779	45.213	47.682	48.892
	90	40.793	43.804	46.898	47.958
CCFF	0	29.312	29.409	29.596	29.413
	15	29.948	30.167	30.551	30.419
	30	31.211	31.548	32.023	31.936
	45	33.377	33.876	34.284	34.270
	60	37.124	37.918	38.165	38.315
	75	42.187	43.812	44.531	45.191
	90	43.943	45.859	49.123	49.343
CFCF	0	16.299	16.419	16.797	16.426
	15	16.320	16.558	17.036	16.765
	30	16.670	17.841	19.477	19.572
	45	17.877	21.341	25.710	26.560
	60	19.715	26.198	33.831	35.551
	75	21.358	30.343	40.613	43.025
	90	22.040	31.967	43.256	45.952

boundary conditions frequency increases with θ . For CCSS and CSCS shells $\theta = 60^\circ$ either gives the highest frequency or yields a frequency value which is marginally less than the highest one. Similarly for SSSS shells $\theta = 75^\circ$ and for CCFF and CFCF shells $\theta = 90^\circ$ gives the highest results.

Figure 5 represents the typical mode shapes corresponding to symmetric cross ply and angle ply laminated composite stiffened shells with cut-out for first five natural modes.

Boundary condition & θ	Mode	(0/0/0)	(0/0) _s	(0/0/0) _s	[(0/0) ₂] _s
CCCC 45°	1				
	2				
	3				
	4				
	5				
CCSS 90°	1				
	2				
	3				
	4				
	5				

FIG. 5. Mode shapes for symmetric cross ply and angle ply shells with cut-out for first five modes.

4.3. Effect of lamination angle between symmetric and antisymmetric laminations on higher mode frequencies

The frequencies of four layered symmetric and antisymmetric laminates are furnished in Table 5 for various lamination angles and boundary conditions. Since four layered laminates are very common in industrial applications, Table 5 is expected to be a good design aid for practicing engineers. Examining the frequencies of shells with four layered symmetric and antisymmetric stacking orders presented in Table 5, it is found that for CFCF shells with 0/θ/0/θ stacking order the vibrational stiffness increase monotonically with θ. But for CCCC, CCSS and SSSS and 0/θ/θ/0 shells, the frequency increases with θ upto a certain value but decreases when θ is further increased. Such decreases are quite marginal in all of these cases. All these observations are true for the first five modes shown

Table 5. Non-dimensional frequencies $\bar{\omega}$ for composite stiffened hypar shell with cut-out with $0/\theta/0/\theta$ and $0/\theta/\theta/0$ lamination scheme and different boundary conditions on higher mode.

θ [°]	Mode	Boundary condition							
		CCCC		CSCS		SSSS		CFCF	
		$0/\theta/0/\theta$	$0/\theta/\theta/0$	$0/\theta/0/\theta$	$0/\theta/\theta/0$	$0/\theta/0/\theta$	$0/\theta/\theta/0$	$0/\theta/0/\theta$	$0/\theta/\theta/0$
0	1	93.093	93.093	39.935	39.935	32.543	32.543	16.419	16.419
	2	106.371	106.371	55.034	55.034	48.270	48.270	33.066	33.066
	3	109.995	109.995	73.047	73.047	56.092	56.092	48.250	48.250
	4	110.260	110.260	87.515	87.515	62.595	62.595	48.520	48.520
	5	116.956	116.956	95.965	95.965	84.479	84.479	56.071	56.071
15	1	111.960	114.779	45.478	43.983	36.699	35.396	16.844	16.558
	2	115.687	116.295	61.772	59.971	54.530	52.559	34.766	33.921
	3	128.878	130.301	81.674	78.304	56.864	57.909	50.135	50.021
	4	130.427	133.877	100.026	101.648	71.059	67.853	52.497	51.119
	5	140.496	142.419	102.962	106.987	92.798	94.828	57.662	56.664
30	1	118.349	122.546	53.234	49.570	42.253	39.215	20.373	17.841
	2	132.432	129.103	75.344	67.956	58.233	58.848	41.158	36.867
	3	146.421	140.195	101.662	88.629	64.897	59.485	55.465	53.783
	4	148.276	152.635	118.461	116.438	87.613	76.774	56.016	55.531
	5	160.833	161.266	122.698	122.225	105.810	103.934	69.109	61.080
45	1	121.010	122.941	61.578	54.464	46.469	42.274	28.739	21.341
	2	136.675	130.152	92.408	76.412	57.809	59.411	52.006	43.288
	3	156.322	140.900	125.669	100.876	75.658	64.370	60.782	60.975
	4	156.944	159.237	128.633	125.125	102.074	85.970	67.482	61.683
	5	166.305	171.106	133.669	132.857	108.272	106.353	85.023	72.540
60	1	119.538	118.771	68.120	58.216	48.447	44.707	39.328	26.198
	2	136.911	126.372	106.292	83.176	56.160	58.318	63.872	52.105
	3	151.622	141.852	123.653	111.838	84.490	68.661	68.950	71.193
	4	163.179	158.797	138.385	123.093	93.730	93.617	84.106	71.841
	5	165.697	161.590	149.906	137.592	119.474	102.556	91.687	85.248
75	1	116.354	113.132	68.504	57.051	48.332	45.213	48.283	30.343
	2	124.902	119.546	106.126	83.470	53.117	56.868	74.826	59.516
	3	138.661	140.262	117.868	115.616	84.436	69.285	79.476	82.918
	4	148.999	143.832	131.935	118.242	89.881	95.616	96.764	82.980
	5	155.419	145.424	132.464	126.783	108.352	97.490	97.422	89.354
90	1	101.746	102.030	65.309	53.208	48.701	43.804	51.795	31.967
	2	117.561	111.696	87.723	77.722	48.995	56.080	71.901	60.044
	3	118.346	127.711	110.525	102.523	80.970	68.019	78.391	80.826
	4	134.043	128.893	115.587	111.379	89.063	90.758	88.043	82.361
	5	151.843	138.257	120.032	114.690	103.765	98.610	100.779	89.747

here except very few cases. In some cases considered here (for CFCF shells with $0/\theta/0/\theta$) highest frequencies are found to be at $\theta = 90^\circ$. In other cases highest frequencies are found to be at $\theta = 60^\circ$.

When performances of antisymmetric and symmetric laminates are compared, it is found that considering all the modes performance of antisymmetric laminate is better than its symmetric counterpart. The only exception is symmetrically laminated CCCC shell with lamination angle 15° . For this shell symmetric laminate perform better than the antisymmetric laminate in all five modes shown here.

Figure 6 represents the typical mode shapes corresponding to symmetric and anti-symmetric cross ply and angle ply laminated composite stiffened shells with cut-out for first five natural modes.

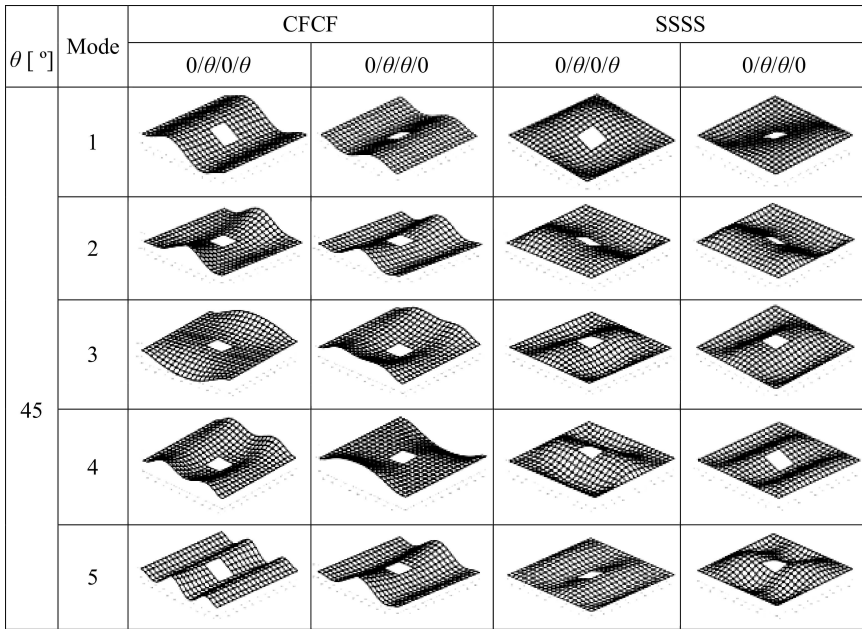


FIG. 6. Mode shapes corresponding to anti symmetric and symmetric laminated composite stiffened hypar shell with cut-out for different boundary conditions for first five modes.

4.4. Effect of curvature on higher mode frequencies

The frequencies of $0/\theta/\theta/0$ laminates are presented in Table 6 for various lamination angles with different c/a ratio for CCSS boundary condition. It is observed in general that frequency of each mode first increases with lamination angle then decrease for all c/a ratios. From Table 6 it is also observed that for CCSS boundary condition for a given lamination angle increase in c/a ratio increases the frequency of each mode.

Table 6. Non-dimensional frequencies $\bar{\omega}$ for $0/\theta/\theta/0$ stiffened hyper shell with cut-out with different c/a ratio for CCSS boundary condition on higher mode.

θ [°]	Mode	c/a			
		0.2	0.15	0.1	0.05
0	1	81.437	68.926	50.845	33.025
	2	84.595	70.089	52.940	36.752
	3	88.777	77.733	62.553	50.804
	4	95.973	80.442	74.440	66.119
	5	103.540	87.336	75.331	71.641
15	1	85.188	76.139	60.664	38.424
	2	90.133	80.995	61.326	41.498
	3	99.544	82.078	73.217	55.059
	4	112.599	94.783	77.307	69.290
	5	119.977	102.417	82.645	72.224
30	1	88.284	80.280	67.962	47.013
	2	97.437	87.112	71.727	48.636
	3	108.153	91.259	79.937	61.777
	4	125.869	112.832	90.117	73.096
	5	135.310	116.351	93.836	76.124
45	1	89.657	80.509	68.059	47.720
	2	102.168	89.685	75.140	52.607
	3	111.560	97.278	83.203	65.001
	4	127.559	112.103	92.107	74.601
	5	141.559	125.170	101.364	83.599
60	1	89.950	78.548	63.700	43.078
	2	102.446	88.382	71.985	49.824
	3	113.423	97.166	80.544	68.703
	4	121.051	108.805	95.209	75.920
	5	143.545	122.901	100.398	83.882
75	1	89.911	75.713	58.137	37.119
	2	99.165	81.321	62.024	45.068
	3	110.513	94.973	81.766	71.083
	4	117.273	102.476	85.903	74.848
	5	127.497	110.154	93.761	80.592
90	1	90.964	74.507	54.050	34.489
	2	96.054	75.982	58.420	44.005
	3	107.634	92.748	79.692	70.108
	4	108.858	95.015	83.706	75.919
	5	123.965	105.420	89.772	79.067

Figure 7 represents the typical mode shapes corresponding to fundamental and first five modes for symmetric angle ply laminated composite stiffened shells with cut-out for different c/a ratio.

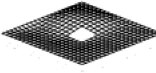
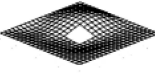
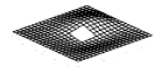
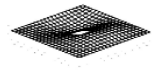
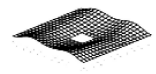
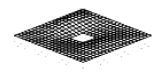
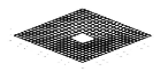
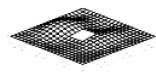
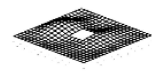
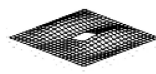
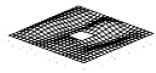
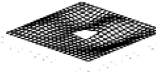
Mode	c/a			
	0.2	0.15	0.1	0.05
1				
2				
3				
4				
5				

FIG. 7. Mode shapes corresponding to 0/45/45/0 laminated composite stiffened hypar shell with cut-out for CCSS boundary conditions for different c/a ratio for first five modes.

5. CONCLUSIONS

The following conclusions are drawn from the present study

- 1) As this approach produces results in close agreement with those of the benchmark problems, the finite element code used here is suitable for analysing the characteristics of vibrating stiffened composite hypars with cut-outs. The present study reveals that cut-outs with stiffened margins may always safely be provided on shell surfaces for functional requirements.
- 2) In general fundamental frequency increases with the increase in the number of support constraints. There are, however, few departures from this general tendency when two shells of different laminations are compared. Sometimes lamination order influences the frequency of stiffened composite shell with cut-out more significantly than its boundary conditions.
- 3) $(0/\theta)_s$ lamination exhibit reasonably good performance and may be adopted for all practical purposes.
- 4) For four layered laminates the frequency either increases monotonically with θ or increases with θ only up to a certain value of θ . For CCCC, CSCS, SSSS and $0/\theta/\theta/0$ CCSS shells, the frequency increases with θ up to a certain value, but decreases when θ is further increased. For each of

these shells the values of θ yielding highest frequencies are to be found out by numerical experimentation. All these observations are true for the first five modes except very few cases.

- 5) Considering all the modes performance of four layered antisymmetric laminate is better than its symmetric counterpart, except CCC shell with lamination angle 15° .
- 6) For shell with CCSS boundary condition, for a given lamination angle, frequency of each mode increases with increase in c/a ratio.

REFERENCES

1. NARITA Y., LEISSA A.W., *Vibrations of corner point supported shallow shells of rectangular planform*, Earthquake Engineering and Structural Dynamics, **12**: 651–661, 1984.
2. REDDY J.N., CHANDRASHEKHARA K., *Geometrically non-linear transient analysis of laminated doubly curved shells*, International Journal of Non-Linear Mechanics, **20**(2): 79–90, 1985.
3. LIEW K.M., KIRTIPORANCHAI S., WANG C.M., *Research developments in analyses of plates and shells*, Journal of Construction Steel Research, **26**(2–3): 231–248, 1993.
4. SCHWARTE J., *Vibrations of corner point supported rhombic hyper-shells*, Journal of Sound and Vibration, **175**(1): 105–114, 1994.
5. CHAKRAVORTY D., BANDYOPADHYAY J.N., SINHA P.K., *Finite element free vibration analysis of point supported laminated composite cylindrical shells*, Journal of Sound and Vibration, **181**(1): 43–52, 1995.
6. QATU M.S., LEISSA A.W., *Vibration studies for laminated composite twisted cantilever plates*, International Journal of Mechanical Sciences, **33**(11): 927–940, 1991.
7. QATU M.S., LEISSA A.W., *Free vibrations of completely free doubly curved laminated composite shallow shells*, Journal of Sound and Vibration, **151**(11): 9–29, 1991.
8. QATU M.S., LEISSA A.W., *Natural frequencies for cantilevered doubly curved laminated composite shallow shells*, Composite Structures, **17**: 227–255, 1991.
9. SIVASUBRAMONIAN B., KULKARNI A.M., RAO G.V., *Free vibration of curved panels with cut-outs*, Journal of Sound and Vibration, **200**(2): 227–234, 1997.
10. LIEW K.M., LIM C.W., *Vibration of perforated doubly curved shallow shells with rounded corners*, International Journal of Solids and Structures, **31**(11): 1519–1536, 1994.
11. LIEW K.M., LIM C.W., *A Pb-2 Ritz formulation for flexural vibration of shallow cylindrical shells of rectangular planform*, Journal of Sound and Vibration, **173**(3): 343–375, 1994.
12. LIEW K.M., LIM C.W., *Vibratory characteristics of cantilever rectangular shallow shells of variable thickness*, AIAA Journal, **32**(2): 387–396, 1994.
13. LIEW K.M., LIM C.W., *A Ritz vibration analysis of doubly curved rectangular shallow shells using a refined first-order theory*, Computer Methods in Applied Mechanics and Engineering, **127**(1–4): 145–162, 1995.

14. LIEW K.M., LIM C.W., *Vibratory behaviour of shallow conical shells by a global Ritz formulation*, Engineering Structures, **17**(1): 63–70, 1995.
15. LIEW K.M., LIM C.W., *Higher-order theory for vibration analysis of cantilever thick shallow shells with constrained boundaries*, Journal of Vibration and Control, **1**(1): 15–39, 1995.
16. LIEW K.M., LIM C.W., *Vibratory characteristics of pre-twisted cantilever trapezoids of unsymmetric laminates*, AIAA Journal, **34**(5): 1041–1050, 1996.
17. LIEW K.M., LIM C.W., ONG L.S., *Vibration of pre-twisted shallow conical shells*, International Journal of Solids and Structures, **31**(18): 2463–2476, 1994.
18. LIEW K.M., LIM C.W., ONG L.S., *Flexural vibration of doubly-tapered cylindrical shallow shells*, International Journal of Mechanical Sciences, **36**(6): 547–565, 1994.
19. LIM C.W., LIEW K.M., *Vibration of pre-twisted cantilever trapezoidal symmetric laminates*, Acta Mechanica, **111**: 193–208, 1995.
20. LIEW K.M., LIM C.W., KITIPORANCHAI S., *Vibration of shallow shells: a review with bibliography*, Applied Mechanics Reviews, **50**(8): 431–444, 1997.
21. CHAKRAVORTY D., BANDYOPADHYAY J.N., SINHA P.K., *Applications of FEM on free and forced vibrations of laminated shells*, ASCE Journal of Engineering Mechanics, **124**(1): 1–8, 1998.
22. SAHOO S., CHAKRAVORTY D., *Finite element vibration characteristics of composite hypar shallow shells with various edge supports*, Journal of Vibration and Control, **11**(10): 1291–1309, 2005.
23. PRADYUMNA S., BANDYOPADHYAY J.N., *Static and free vibration analyses of laminated shells using a higher-order theory*, Journal of Reinforced Plastics and Composites, **27**: 167–186, 2008.
24. RIKARDS R., CHATE A., OZOLINSH O., *Analysis for buckling and vibrations of composite stiffened shells and plates*, Composite Structures, **51**: 361–370, 2001.
25. NAYAK A.N., BANDYOPADHYAY J.N., *Free vibration analysis and design aids of stiffened conoidal shells*, ASCE Journal of Engineering Mechanics, **128**(4): 419–427, 2002.
26. NAYAK A.N., BANDYOPADHYAY J.N., *On the free vibration of stiffened shallow shells*, Journal of Sound and Vibration, **255**(2): 357–382, 2002.
27. NAYAK A.N., BANDYOPADHYAY J.N., *Free vibration analysis of laminated stiffened shells*, ASCE Journal of Engineering Mechanics, **131**(1): 100–105, 2005.
28. NAYAK A.N., BANDYOPADHYAY J.N., *Dynamic response analysis of stiffened conoidal shells*, Journal of Sound and Vibration, **291**(3–5): 1288–1297, 2006.
29. SAHOO S., CHAKRAVORTY D., *Finite element vibration characteristics of composite hypar shallow shells with various edge supports*, Journal of Vibration and Control, **11**(10): 1291–1309, 2005.
30. SAHOO S., CHAKRAVORTY D., *Stiffened composite hypar shell roofs under free vibration, behaviour and optimization aids*, Journal of Sound and Vibration, **295**(1–2): 362–377, 2006.
31. KUMAR A., BHARGAVA P., CHAKRABARTI A., *Natural frequencies and mode shape of laminated composite skew hypar shells with complicated boundary conditions using finite element method*, Advanced Material Research, **585**: 44–48, 2012.

32. KUMAR A., BHARGAVA P., CHAKRABARTI A., *Vibration of laminated composite skew hyper shells using higher order theory*, Thin Walled Structures, **63**: 82–90, 2013.
33. KUMAR A., CHAKRABARTI A., BHARGAVA P., *Vibration analysis of laminated composite skew cylindrical shells using higher order shear deformation theory*, Journal of Vibration and Control, **21**(4): 725–735, 2015.
34. GULSHANTAJ M.N.A., CHAKRABARTI A., *Dynamic response of functionally graded skew shell panel*, Latin American Journal of Solids and Structures, **10**(6): 1243–1266, 2013.
35. TORNABENE F., FANTUZZI N., BACCIOCCHI M., DIMITRI R., *Dynamic analysis of thick and thin elliptic shell structures made of laminated composite materials*, Composite Structures, **133**: 278–299, 2015.
36. DEY S., MUKHOPADHYAY T., ADHIKARI S., *Stochastic free vibration analyses of composite shallow doubly curved shells – A Kriging model approach*, Composite: Part B, **70**: 99–112, 2015.
37. ZHANG C., JIN G., MA X., YE T., *Vibration analysis of circular cylindrical double-shell structures under general coupling and end boundary conditions*, Applied Acoustics, **110**: 176–193, 2016.
38. SAHOO S., *Behaviour and optimization aids of composite stiffened hyper shell roofs with cutout under free vibration*, ISRN Civil Engineering, ID 989785, 1–14, 2012.
39. SAHOO S., *Dynamic characters of stiffened composite conoidal shell roofs with cut-outs: Design aids and selection guidelines*, Journal of Engineering, ID 230120, 1–18, 2013.
40. SAHOO S., *Free vibration of laminated composite stiffened saddle shell roofs with cut-outs*, IOSR Journal of Mechanical and Civil Engineering, ICAET-2014, 30–34, 2014.
41. SAHOO S., *Laminated composite stiffened shallow spherical panels with cut-outs under free vibration – a finite element approach*, Engineering Science and Technology, An International Journal, **17**(4): 247–259, 2014.
42. SAHOO S., *Free vibration behavior of laminated composite stiffened elliptic paraboloidal shell panel with cut-out*, Curved and Layered Structures, **2**(1): 162–182, 2015.
43. SAHOO S., *Laminated composite stiffened cylindrical shell panels with cut-outs under free vibration*, International Journal of Manufacturing, Materials, and Mechanical Engineering, **5**(3): 37–63, 2015.
44. SAHOO S., *Performance evaluation of free vibration of laminated composite stiffened hyperbolic paraboloid shell panel with cut-out*, International Journal of Engineering and Technologies, **7**: 1–24, 2016.
45. TOPAL U., *Mode-frequency analysis of laminated spherical shell*, [in:] Proceedings of the 2006 IJME. INTERTECH International Conference-Session ENG P501-001, Kean University, NJ; 19–21 October, 2006.
46. SRINIVASA C.V., SURESH Y.J., PREMA KUMAR W.P., *Experimental and finite element studies on free vibration of cylindrical skew panels*, International Journal of Advanced Structural Engineering, **6**(1), 2014, doi: 10.1186/2008-6695-6-1.
47. DEY S., MUKHOPADHYAY T., SAHU S.K., ADHIKARI S., *Effect of cut-out on stochastic natural frequency of composite curved panels*, Composites Part B: Engineering, **105**: 188–202, 2016.

48. VASILIEV V.V., JONES R.M., MAN L.L., *Mechanics of composite structures*, Taylor and Francis, USA, 1993.
49. QATU M.S., *Vibration of laminated shells and plates*, Elsevier, UK, 2004.
50. DEY A., BANDYOPADHYAY J.N., SINHA P.K., *Finite element analysis of laminated composite conoidal shell structures*, *Computers and Structures*, **43**(30): 469–476, 1992.
51. MUKHERJEE A., MUKHOPADHYAY M., *Finite element free vibration of eccentrically stiffened plates*, *Computers and Structures*, **30**(6): 1303–1317, 1988.
52. DEY A., BANDYOPADHYAY J.N., SINHA P.K., *Finite element analysis of laminated composite paraboloid of revolution shells*, *Computers and Structures*, **44**(3): 675–682, 1992.

Received July 27, 2018; accepted version January 7, 2019.

Published on Creative Common licence CC BY-SA 4.0

